Electronic Supplementary Information for

Insights into biochar supported atomically dispersed cobalt as an efficient peroxymonosulfate activator for sulfamethoxazole degradation: Robust performance, ROS and surface electron-transfer pathways

Chunyao Gu[a], Yaqin Zhang[b], Peng He[a], Jianyu Zhu[a]*, Min Gan[a]*

a. School of Minerals Processing and Bioengineering, Key Laboratory of Biohydrometallurgy of Ministry of Education, Central South University, Changsha 410083, China.

b. Laboratory of Micro & Nano Biosensing Technology in Food Safety, Hunan Provincial Key Laboratory of Food Science and Biotechnology, College of Food Science and Technology, Hunan Agricultural University, Changsha 410128, China.

*Corresponding authors at: School of Minerals Processing and Bioengineering, Central South University, South Lushan Road 932, Changsha, Hunan 410083, People's Republic of China. Tel: +86-13755146512 (Jianyu Zhu) and +86-18373143548 (Min Gan). E-mail address: zhujy@csu.edu.cn (Jianyu Zhu) and ganmin0803@csu.edu.cn (Min Gan).

Submitted to

Environmental Science: Nano

Experimental Section

Chemicals and reagents. Manganese (II) acetate tetrahydrate, cobalt (II) acetate tetrahydrate, nickel (II) acetate tetrahydrate, Rhodamine B (RhB), methyl orange (MO), methyl blue (MB), and 1,10-phenanthroline monohydrate were purchased from Sinopharm Chemical Reagent Co., Ltd., China. Iron (II) acetate (>90.0% (T)), sulfamethoxazole (SMX, 98%), p-benzoquinone (p-BQ), furfuryl alcohol (FFA), tetracycline (TC), Ciprofloxacin (CIP), and peroxymonosulfate (PMS) were provided from Sigma-Aldrich, USA. Methanol (MeOH), ethanol, tert-Butanol (TBA), L-histidine, potassium nitrate, potassium sulfate, potassium dihydrogen phosphate, potassium chloride, sodium hydrogen carbonate, potassium iodide, hydrochloric acid, sulfuric acid, and sodium hydroxide were obtained from Sinopharm Chemical Reagent Co., Ltd., China. 5,5-dimethyl-1-pyrolin-N-oxide (DMPO ≥ 97%) and 2,2,6,6-tetramethylpiperidine (TEMP, 98%) were purchased from Sigma-Aldrich, USA. All chemicals were of analytical grade and used without further purification.

Preparation of biochar. The rice straw was obtained in Changsha city, Hunan province, China, and it was pyrolyzed to yield biochar. Before the pyrolysis, the rice straw was cut into small pieces, washed with deionized water several times, and then dried in oven at 100 ℃ for 24 hours. The dried rice straw was ground into powder by domestic mill and passed through a 160-mesh sieve. According to previous reports,[1] the powder was transferred into a laboratory scale tube furnace, heated at 10 ℃ min^{-1} to 900 ℃ under 200 cm^3 min^{-1} CO_2 flow rate for 2 hours. After cooling to room temperature, the pyrolysis products were treated with 1 M HCl for 2 hours, washed with deionized water until the pH was near neutral, and dried in oven at 60 ℃ overnight.

Preparation of Me-N@BC catalysts. Briefly, acetate complexed with 1,10-phenanthroline in ethanol solvent, mixed and dried with the prepared biochar, and calcined in a tube furnace.[2] 1.0 mM acetate and 3.0 mM 1, 10-phenanthroline were dissolved into 50 mL ethanol with ultrasonication for 10 minutes, and then added 0.9 g of the prepared biochar sonicate to disperse for another 20 minutes. The mixed solution

was evaporated to dryness in a water bath at 60 ℃ under continuous magnetic stirring. Subsequently, the resulting dispersion was heated at 80 ℃ in oven overnight to complete the evaporation of ethanol. The dried solid was ground into a fine powder and then annealed under argon atmosphere at 600°C with a heat rate of 10 °C·min^{-1} and maintained for 2 hours under 100 cm^3 min^{-1} flow rate. The biochar-supported transition metal catalysts (Me-N@BC) were yielded after cooling to room temperature and were denoted as Mn-N@BC, Fe-N@BC, 1.0-Co-N@BC, and Ni-N@BC, respectively. For comparison, 1,10-phenanthroline and biochar were mixed and calcined to obtain metal-free material (Phen@BC), and biochar was reannealed to obtain r-BC. The other steps were the same as above.

Preparation of Co-N@BC catalysts. Co-N@BC catalysts were prepared using the same procedure. The dose of cobalt (II) acetate was changed to 0.1 mM, 0.25 mM, 0.5 mM, and 2.0 mM, and the dose of 1,10-phenanthroline was proportionally changed to 0.3 mM, 0.75 mM, 1.5 mM, and 6.0 mM, respectively. The products were yielded after anneal and named as 0.1-Co-N@BC, 0.25-Co-N@BC, 0.5-Co-N@BC, and 2.0-Co-N@BC, respectively.

Materials characterization. The crystalline was observed by X-ray diffraction (XRD, XRD-6000, SHIMADZU, Japan) using a Cu Kα radiation source. The morphology and structure were explored by scanning electron microscopy (FE-SEM, TESCAN MIRA3 LMH/LMU, Czech), transmission electron microscopy (TEM, FEI tencnai G2F20 S-Twin, USA), and high-angle annular dark-field scanning transmission electron microscopy (HAADF-STEM, JEM-ARM-200F, Japan). An X–ray photoelectron spectrometer (XPS, EscaLab Xi+, ThermoFischer, USA) was employed to analyze the surface chemical compositions and the element valence state under the Al Ka X-ray source condition. The degree of graphitization was analyzed by Raman spectrum (Raman, inVia, Renishaw, UK). The electrochemical property of all the prepared samples was detected by electrochemical workstation (CHI760E, Shanghai Chenhua Instrument Co, China). Electron paramagnetic resonance (EPR, Bruker A300,

Germany) was used to directly detect DMPO-$SO_4^{\cdot-}$, DMPO-$OH^{\cdot}$, and DMPO-$O_2^{\cdot-}$ with DMPO as the spin-trapping agent, while TEMP-$^1O_2$ with TEMP as the spin-trapping agent.

Experimental procedures. The SMX degradation was employed to evaluate the performance of the biochar supported atomically-dispersed cobalt catalysts in PMS activation. Batch experiments were conducted in a 150 mL flask with continuous stirring (600 rpm) at 30±1 ℃. Typically, the prepared catalyst (5 mg) was dispersed in a 45 mL SMX solution, and then a certain amount of PMS solution was introduced to trigger the reaction. At time intervals, the reaction solution was extracted and injected into sufficient methanol to quench the reaction. The resulting solution was filtrated by a 0.22 μm syringe filter. In the quenching tests, MeOH, TBA, p-BQ, FFA, and L-histidine were used as scavengers to investigate the main active species in the 0.5-Co-N@BC/PMS system. H_2SO_4, NaOH or phosphate buffer were used to adjust the desired pH value. All experiments were carried out in ultrapure water and conducted in duplicate.

Analytical methods. The concentration of SMX was detected by high-performance liquid chromatography (HPLC, SHIMADZU, Japan) equipped with a C-18 column (Shim-pack GIST, 5 μm, 4.6X250 mm). The mobile phase was a mixture of Acetonitrile: Water (pH=2.5, phosphoric acid) (70/30, v/v) with a flow rate of 0.5 mL min^{-1}, and it was detected at wavenumber of 270 nm.[3] The cobalt leaching was observed by ICP-OES (ICP-OES, Spectro Blue II, SPECTRO, Germany). The consumption of PMS was measured using the modified iodometric titration method by a UV–vis spectrophotometer (UV-1780, SHIMADZU, Japan) at 352 nm.[4] The concentration of RhB,MO, MB, TC and CIP was determined by measuring the absorbance at 554, 464, 664, 360, and 273 nm using a microplate reader (Epoch, BioTek, USA)/ UV–vis spectrophotometer, respectively. Total organic carbon (TOC) was determined by a Total Organic Carbon Analyzer (Jena Multi N/C 3100, Germany). The SMX products

was investigated by an Agilent 1290 Infinity ultra-high performance liquid chromatography system coupled with an Agilent 6550 quadrupole time-of-flight mass spectrometry (UPLC/Q-TOF-MS, Agilent Technologies, USA).

Electrochemical measurements. The electrochemical properties of Co-N@BC were evaluated on an electrochemical workstation with three electrode cells. The electrolyte was composed of 50 mM Na_2SO_4 and 0.4 mM PMS, with the $Hg/HgCl_2$ electrode as the reference electrode and the platinum as the auxiliary electrode. To prepare the working electrode, 50 mg of Co-N@BC catalysts were introduced into 1 mL of deionized water and were dispersed uniformly with ultrasound. 70 μL sample solution was mixed with 30 μL of Nafion solution (5 wt%) by ultrasonic dispersion, then 7 μL of the catalyst suspension was injected into the working electrode and dried at room temperature. Cyclic voltammetry was performed as the potential varied from -1.4 to 1.4 V vs. $Hg/HgCl_2$ with a scan rate of 0.05 V/s. Linear-sweep voltammograms were gained as the potential varied from 0 to 1.0 V vs. $Hg/HgCl_2$ with a scan rate of 0.05 V/s. Electrochemical impedance plots were acquired at open circuit potential vs. $Hg/HgCl_2$ with a frequency range from 10^5 to 10^{-2} Hz, utilizing an AC voltage at 0.005 V amplitude.

Text. S1 Chemical reaction equations

The generation and activation equations of SO_5^{2-}.

$$HSO_5^- + OH^- \rightarrow SO_5^{2-} + H_2O \quad (1)$$

$$Co(II) + SO_5^{2-} + H_2O \rightarrow Co(III) + SO_4^{\cdot -} + 2OH^- \quad (2)$$

The formation of chlorine-containing reactive oxygen species.

$$Cl^- + SO_4^{\cdot -} \rightarrow Cl^{\cdot} + SO_4^{2-} \quad (3)$$

$$Cl^- + OH^{\cdot} \rightarrow ClHO^{\cdot -} \quad (4)$$

$$ClHO^{\cdot -} + H^+ \rightarrow Cl^{\cdot} + H_2O \quad (5)$$

$$Cl^- + Cl^{\cdot} \rightarrow Cl^{\cdot}{}_2^-$$ (6)

$$Cl^- + HSO_5^- \rightarrow SO^2{}_4^- + HOCl$$ (7)

The generation of nitrate radicals.

$$NO_3^- + SO^{\cdot}{}_4^- \rightarrow SO^2{}_4^- + NO_3^{\cdot}$$ (8)

$$NO_3^- + OH^{\cdot} \rightarrow OH^- + NO_3^{\cdot}$$ (9)

The ionization equilibrium equation of SMX.[5]

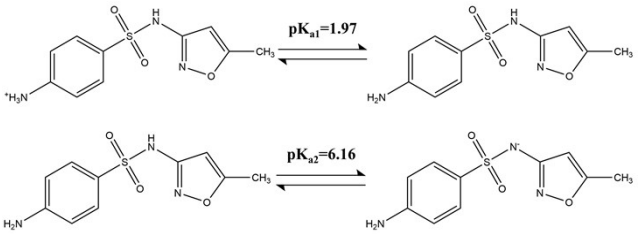

(10)

(11)

Table. S1 Surface element composition of Co-N@BC.

Sample	Content (at%)			
	C1s	N1s	O1s	Co2p
0.1-Co-N@BC	56.64	2.29	40.63	0.44
0.25-Co-N@BC	62.85	3.94	32.65	0.57
0.5-Co-N@BC	69.29	5.28	24.85	0.57
1.0-Co-N@BC	73.01	4.61	21.46	0.61
2.0-Co-N@BC	75.34	6.06	17.91	0.69

Table. S2 The ratio of octahedral and tetrahedral Co in Co-N@BC.

Sample	Co Content (%)	
	Octahedral Co	Tetrahedral Co
0.1-Co-N@BC	36.70	63.30
0.25-Co-N@BC	47.56	52.44
0.5-Co-N@BC	60.41	39.59
1.0-Co-N@BC	54.19	45.81
2.0-Co-N@BC	50.74	49.26
0.5-Co-N@BC after reaction	58.76	41.24

Table. S3 The ratio of different N species in Co-N@BC.

Sample	N Content (at%)		
	Pyridinic N	Pyrrolic N	Graphitic N
0.1-Co-N@BC	32.29	27.23	40.47
0.25-Co-N@BC	47.55	27.58	24.87
0.5-Co-N@BC	47.40	29.93	22.67
1.0-Co-N@BC	56.99	21.46	21.54
2.0-Co-N@BC	61.46	18.32	20.22
0.5-Co-N@BC after reaction	58.74	24.40	16.86

Table. S4 The performance comparison of recently reported catalysts on PMS activation for SMX degradation.

No.	Material	SMX (μM)	PMS (mM)	Cata (g L^{-1})	Time (min)	Kobs (min^{-1})	TOF (min^{-1})	Degradation rate	Ref
1	α-Fe_2O_3-VO	10	0.1	0.1	60	0.0403	0.403	91.5%	6
2	NRGO	40	0.8	0.5	240	0.0101	0.0202	91.7%	7
3	Co-NP	9.87	0.15	0.1	60	0.0644	0.644	100%	8
4	40MF	39.48	0.329	0.2	40	0.067	0.335	92.9%	9
5	Ag_2O-Ag eggshell	39.48	0.16	0.1	60	0.0877	0.877	94.67%	10
6	nano-bim Co/Fe oxides	40	0.4	0.2	60	0.057	0.285	100%	11
7	FeO_y/S-g-C_3N_4	39.48	0.8	0.5	90	0.06	0.12	100%	12
8	Fe-Co-O-g-C_3N_4	40	0.8	0.2	30	0.085	0.425	100%	13
9	Se-g-C_3N_4	39.48	1.301	0.2	180	0.0149	0.0745	93.0%	14
10	MF	39.48	0.813	0.06	40	0.05088	0.848	90%	15
11	PAN-Co-C	39.48	0.325	2.0	60	0.113	0.0565	99.3%	16
12	CT1%Cu_2O	6.32	0.065	0.2	60	0.0079	0.0395	42%	17
13	**0.5-Co-N@BC**	**39.48**	**0.4**	**0.1**	**60**	**0.12665**	**1.2665**	**99.6%**	**This work**

Table. S5 The accurate mass and structures of SMX and its degradation products.

Product ID and chemical formula	Structure	Measured accurate (m/z)	t_r (min)
SMX	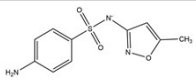	252.07	5.687
P1	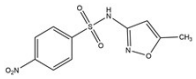	282.13	8.482
P2	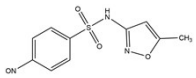	267.98	7.368
P3	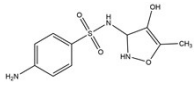	274.22	8.977
P4	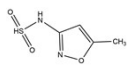	164.93	12.187
P5	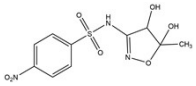	318.42	8.977
P6	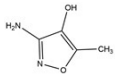	114.09	7.121
P7	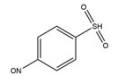	171.16	7.121
P8	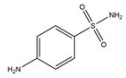	173.16	11.082
P9	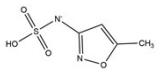	178.96	5.687
P10	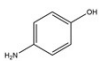	111.04	11.082
P11	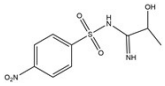	274.22	8.977
P12	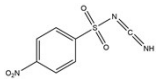	225.10	11.082
P13	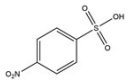	206.96	11.082
P14		137.96	6.368
P15	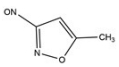	113.11	6.368

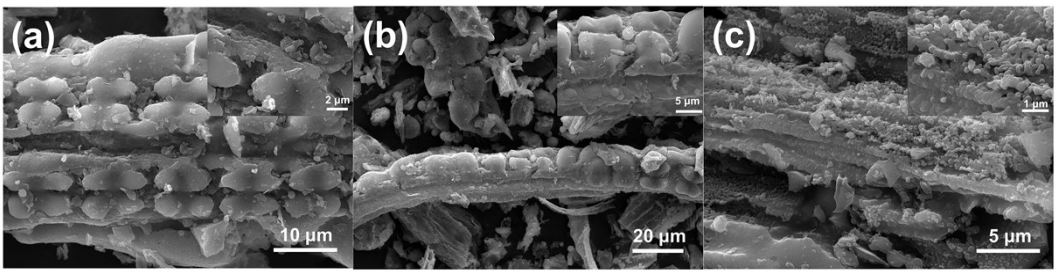

Fig. S1 SEM images of (a) BC, (b) r-BC, and (c) Phen@BC.

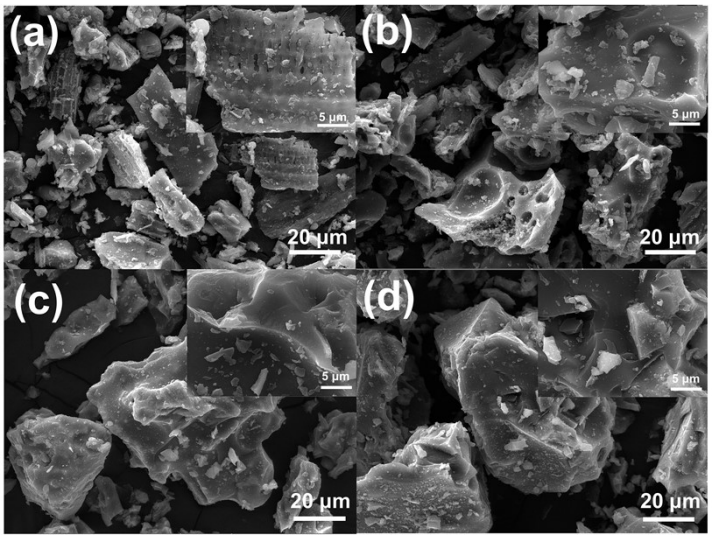

Fig. S2 SEM images of (a) 0.1-Co-N@BC, (b) 0.25-Co-N@BC; (c) 1.0-Co-N@BC, and (d) 2.0-Co-N@BC.

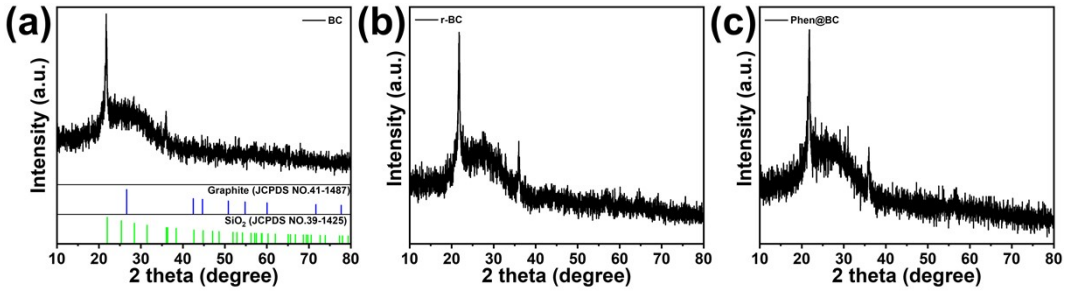

Fig. S3 XRD patterns of (a) BC, (b) r-BC, and (c) Phen@BC.

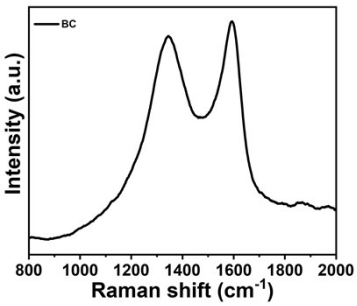

Fig. S4 Raman spectra of BC.

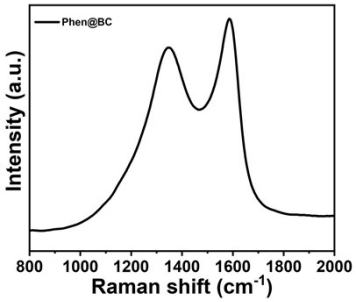

Fig. S5 Raman spectra of Phen@BC.

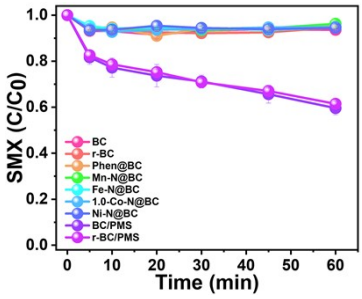

Fig. S6 SMX degradation under different conditions. Experimental condition: [SMX] = 39.48 μM, [Cata] = 0.1 g L^{-1}, [PMS] = 0.4 mM, and pH = 6.8.

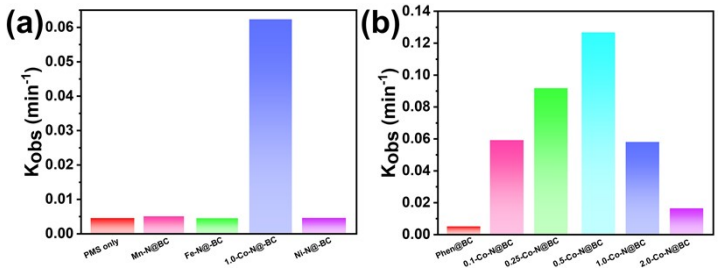

Fig. S7 (a) Reaction rate constant of Me-N@BC on PMS activation; (b) Reaction rate constant of Co-N@BC on PMS activation. Experimental condition: [SMX] = 39.48 μM, [Cata] = 0.1 g L^{-1}, [PMS] = 0.4 mM, and pH = 6.8.

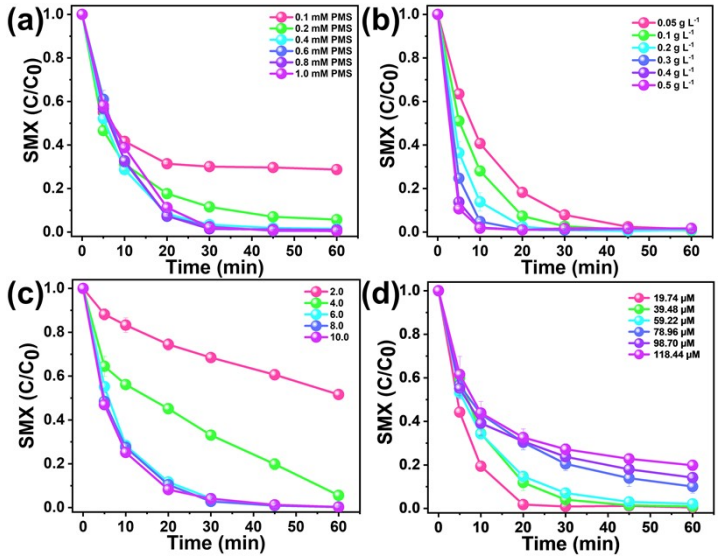

Fig. S8 (a) Effect of PMS dosage; (b) Effect of catalyst dosage; (c) Effect of initial pH in phosphate buffer; (d) Effect of SMX concentration.

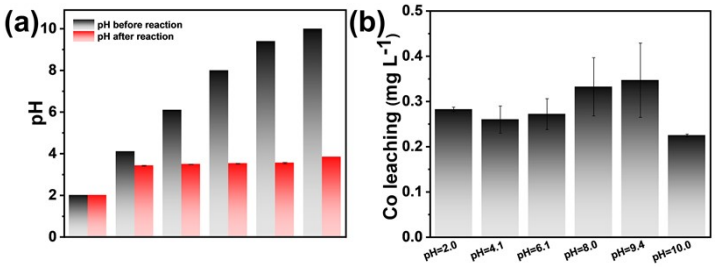

Fig. S9 (a) The solution pH change under different initial pH systems; (b) The Co leaching under different initial pH systems. Experimental condition: [SMX] = 39.48 μM, [Cata] = 0.1 g L^{-1}, [PMS] = 0.4 mM, and pH = 6.8.

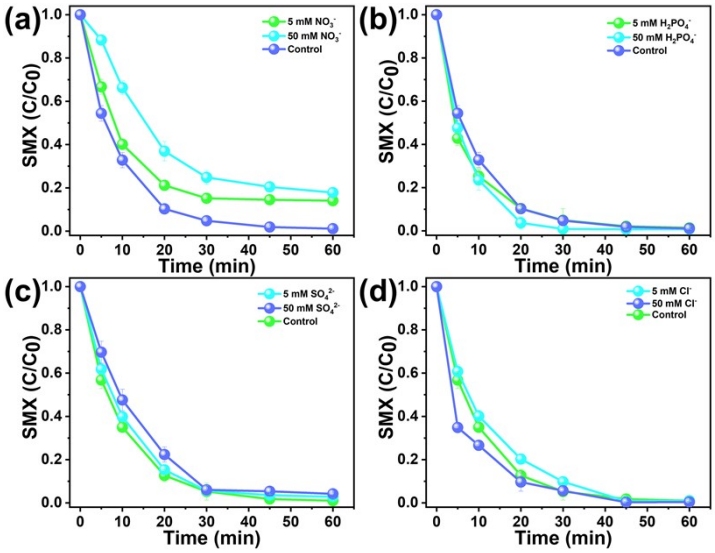

Fig. S10 Effect of different anions (a) NO_3^-, (b) $H_2PO_4^-$, (c) SO_4^{2-}, and (d) Cl^- on SMX degradation. Experimental condition: [SMX] = 39.48 μM, [Cata] = 0.1 g L^{-1}, and [PMS] = 0.4 mM, and pH = 6.8.

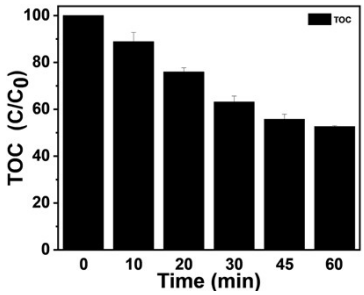

Fig. S11 TOC removal efficiency. Experimental condition: [SMX] = 39.48 μM, [Cata] = 0.1 g L^{-1}, [PMS] = 0.4 mM, and pH = 6.8.

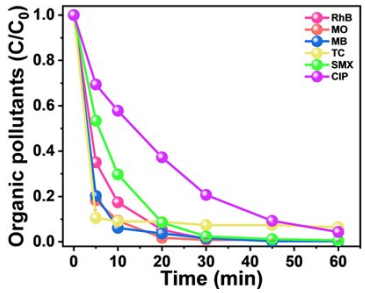

Fig. S12 Degradation of various organic pollutants. Experimental condition: [RhB, MO, MB, TC, CIP, SMX] = 10 mg L^{-1}, [Cata] = 0.1 g L^{-1}, [PMS] = 0.4 mM.

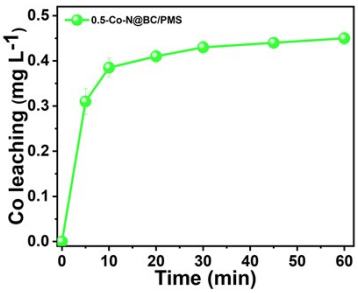

Fig. S13 Co leaching under PMS activation performance. Experimental condition: [SMX] = 39.48 μM, [Cata] = 0.1 g L^{-1}, [PMS] = 0.4 mM, and pH = 6.8.

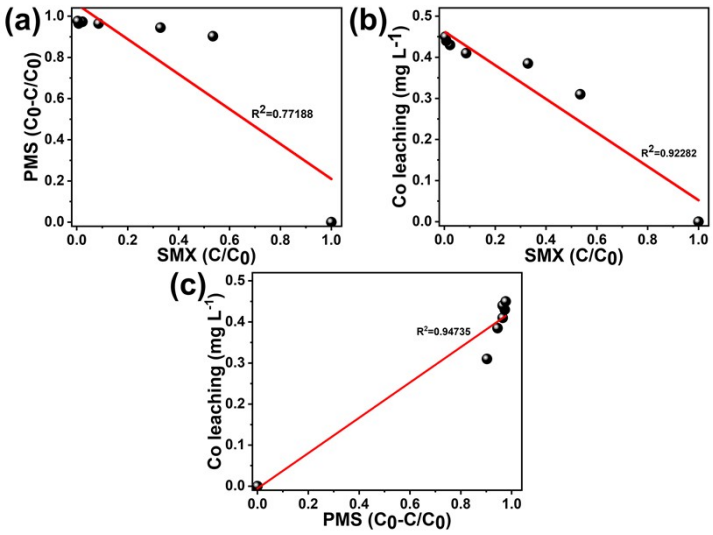

Fig. S14 (a) Correlation analysis of PMS consumption and SMX degradation; (b) Correlation analysis of Co leaching and SMX degradation; (c) Correlation analysis of Co leaching and PMS consumption.

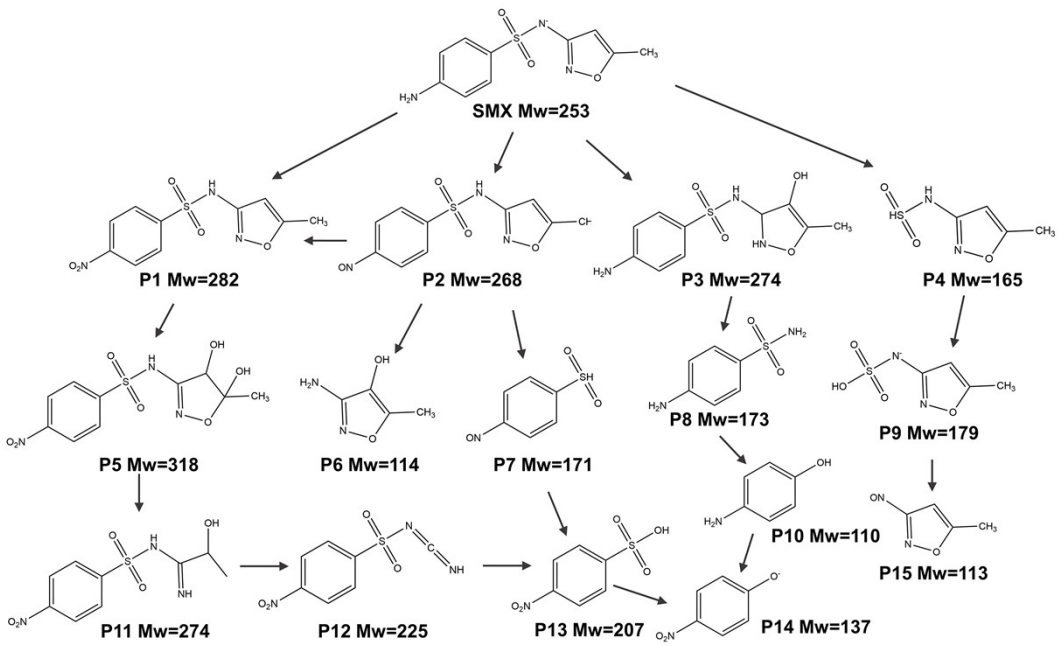

Fig. S15 The proposed SMX degradation pathways in the 0.5-Co-N@BCPMS system.

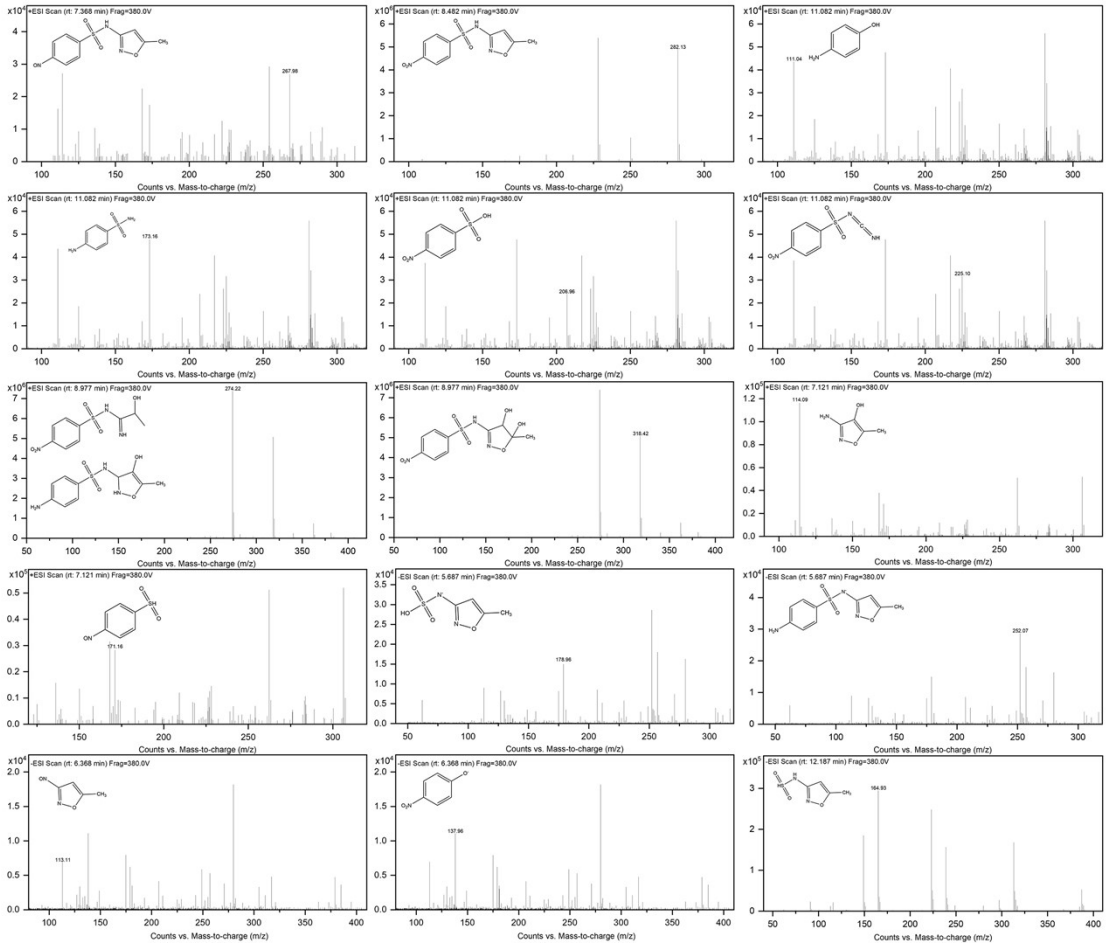

Fig. S16 The MS spectrum of the degradation products of SMX.

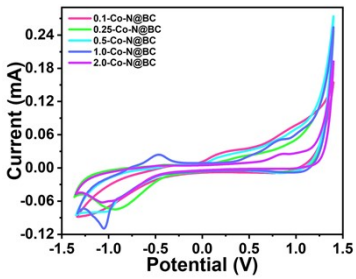

Fig. S17 Cyclic voltammetry of Co-N@BC.

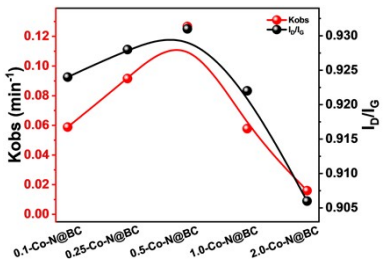

Fig. S18 Relationships of I_D/I_G and kinetic *k* values in Co-N@BC.

References

1. K. Yang, J. Peng, H. Xia, L. Zhang, C. Srinivasakannan and S. Guo, Textural characteristics of activated carbon by single step CO2 activation from coconut shells, *J. Taiwan Inst. Chem. E*, 2010, **41**, 367-372.
2. H. Yang, L. Shang, Q. Zhang, R. Shi, G. I. N. Waterhouse, L. Gu and T. Zhang, A universal ligand mediated method for large scale synthesis of transition metal single atom catalysts, *Nat. Commun.*, 2019, **10**, 4585.
3. Y. Shang, C. Chen, P. Zhang, Q. Yue, Y. Li, B. Gao and X. Xu, Removal of sulfamethoxazole from water via activation of persulfate by Fe3C@NCNTs including mechanism of radical and nonradical process, *Chem. Eng. J.*, 2019, **375**, 122004.
4. C. Liang, C.-F. Huang, N. Mohanty and R. M. Kurakalva, A rapid spectrophotometric determination of persulfate anion in ISCO, *Chemosphere*, 2008, **73**, 1540-1543.
5. H. Milh, B. Schoenaers, A. Stesmans, D. Cabooter and R. Dewil, Degradation of sulfamethoxazole by heat-activated persulfate oxidation: Elucidation of the degradation mechanism and influence of process parameters, *Chem. Eng. J.*, 2020, **379**, 122234.
6. Q. Qin, T. Liu, J. Zhang, R. Wei, S. You and Y. Xu, Facile synthesis of oxygen vacancies enriched α-Fe2O3 for peroxymonosulfate activation: A non-radical process for sulfamethoxazole degradation, *J. Hazard. Mater.*, 2021, **419**, 126447.
7. S. Wang, L. Xu and J. Wang, Nitrogen-doped graphene as peroxymonosulfate activator and electron transfer mediator for the enhanced degradation of sulfamethoxazole, *Chem. Eng. J.*, 2019, **375**, 122041.
8. F. Liu, H. Zhou, Z. Pan, Y. Liu, G. Yao, Y. Guo and B. Lai, Degradation of sulfamethoxazole by cobalt-nickel powder composite catalyst coupled with peroxymonosulfate: Performance, degradation pathways and mechanistic consideration, *J. Hazard. Mater.*, 2020, **400**, 123322.
9. X. Xu, R. Lin, X. Deng and J. Liu, In situ synthesis of FeOOH-coated trimanganese tetroxide composites catalyst for enhanced degradation of sulfamethoxazole by peroxymonosulfate activation, *Sep. Purif. Technol.*, 2021, **275**, 119184.
10. Y. Gao, Q. Zhao, Y. Li, Y. Li, J. Gou and X. Cheng, Degradation of sulfamethoxazole by peroxymonosulfate activated by waste eggshell supported Ag2O-Ag nano–particles, *Chem. Eng. J.*, 2021, **405**, 126719.
11. Y. Bao, W.-D. Oh, T.-T. Lim, R. Wang, R. D. Webster and X. Hu, Elucidation of stoichiometric efficiency, radical generation and transformation pathway during catalytic oxidation of sulfamethoxazole via peroxymonosulfate activation, *Water Res.*, 2019, **151**, 64-74.
12. S. Wang, Y. Liu and J. Wang, Iron and sulfur co-doped graphite carbon nitride (FeOy/S-g-C3N4) for activating peroxymonosulfate to enhance sulfamethoxazole degradation, *Chem. Eng. J.*, 2020, **382**, 122836.
13. S. Wang, Y. Liu and J. Wang, Peroxymonosulfate Activation by Fe–Co–O-Codoped Graphite Carbon Nitride for Degradation of Sulfamethoxazole, *Environ. Sci. Technol.*, 2020, **54**, 10361-10369.
14. Y. Tian, X. Tian, W. Zeng, Y. Nie, C. Yang, C. Dai, Y. Li and L. Lu, Enhanced peroxymonosulfate decomposition into OH and 1O2 for sulfamethoxazole degradation over Se doped g-C3N4 due to induced exfoliation and N vacancies formation, *Sep. Purif. Technol.*, 2021, **267**, 118664.
15. R. Guo, Y. Wang, J. Li, X. Cheng and D. D. Dionysiou, Sulfamethoxazole degradation by visible light assisted peroxymonosulfate process based on nanohybrid manganese dioxide incorporating ferric

oxide, *Appl. Catal., B*, 2020, **278**, 119297.

16. Y. Bao, Y. S. Tay, T.-T. Lim, R. Wang, R. D. Webster and X. Hu, Polyacrylonitrile (PAN)-induced carbon membrane with in-situ encapsulated cobalt crystal for hybrid peroxymonosulfate oxidation-filtration process: Preparation, characterization and performance evaluation, *Chem. Eng. J.*, 2019, **373**, 425-436.
17. Y. Feng, C. Liao, H. Li, C. Liu and K. Shih, Cu2O-promoted degradation of sulfamethoxazole by α-Fe2O3-catalyzed peroxymonosulfate under circumneutral conditions: synergistic effect, Cu/Fe ratios, and mechanisms, *Environ. Technol.*, 2018, **39**, 1-11.